Inorg. Chem. **2003**, *42*, 1151–1157

Nickel(II) Macrocyclic Complexes with Long Alkyl Pendant Chain: Synthesis, X-ray Structure, and Anion Exchange Property in the Solid State

Hye Jin Choi and Myunghyun Paik Suh*

School of Chemistry and Molecular Engineering, and the Center for Molecular Catalysis, Seoul National University, Seoul 151-747, Republic of Korea

Received August 23, 2002

A nickel(II) pentaaza macrocyclic complex containing a 1-hexadecyl pendant chain, $[Ni(C_{25}H_{55}N_5)](ClO_4)_2 \cdot H_2O$ (**1**), was synthesized by a one-pot metal-template condensation reaction. Crystal data for **1**: triclinic, $P\bar{1}$, $a = 8.333(4)$ Å, $b = 8.356(3)$ Å, $c = 28.374(9)$ Å, $\alpha = 81.865(19)°$, $\beta = 86.242(18)°$, $\gamma = 63.871(17)°$, $Z = 2$. Solid **1** forms hydrophobic layers that are constructed by the long alkyl chains of the macrocycles. Solid **1** exchanges ClO_4^- with NCS^-, PF_6^-, $C_2O_4^{2-}$, NO_3^-, and $CF_3SO_3^-$ that are dissolved in water. From the reaction of $[Ni(C_{25}H_{55}N_5)Cl_2]$ with $Et_3NH(TCNQ)_2$ in EtOH/DMF/acetone solution, $[Ni(C_{25}H_{55}N_5)(TCNQ)_2](TCNQ) \cdot (CH_3COCH_3)$ (**2**) (TCNQ = 7,7,8,8-tetracyano-*p*-quinodimethane) was prepared. Crystal data for **2**: triclinic, $P\bar{1}$, $a = 8.459(0)$ Å, $b = 13.945$ (1) Å, $c = 26.833(2)$ Å, $\alpha = 88.744(2)°$, $\beta = 84.536(2)°$, $\gamma = 80.089(4)$ °, $Z = 2$. In **2**, TCNQ anions coordinate nickel(II) at the axial sites, which form π-stacked $TCNQ^-$ dimers to give rise to 1-D chains. The neutral TCNQ molecules are included between the dimerized $TCNQ^-$ species, which construct a π-stacked group of six TCNQ units as blocked by the long alkyl chains. Compound **2** is an electric insulator. It shows a weak signal in the EPR spectrum. The magnetic susceptibility data of **2** measured at 5–300 K exhibit a simple paramagnetism at low temperatures (<100 K) but an increase in the magnetic moment at higher temperatures due to the contribution of a thermally accessible triplet state for the antiferromagnetically coupled $[TCNQ]_2^{2-}$.

Introduction

Organic compounds with long alkyl chains have been extensively employed in self-assembled monolayers,[1] nanoparticles,[2] mesoporous materials,[3] and insulating materials for superconducting monolayers.[4] In addition, self-organization of organic molecules via hydrophobic interactions has been applied to build supramolecular architectures of well-defined shapes and functions.[5,6]

A few transition metal complexes with long alkyl chains have been reported,[7−12] and some of them were isolated from the solution and characterized by X-ray crystallography. Furthermore, some showed improved catalytic activity in water for organic reactions such as the Diels−Alder reaction, hydrolysis, and substitution reaction, by formation of micellar structure.[9,10]

Metal complexes of TCNQ (7,7,8,8-tetracyano-*p*-quinodimethane) have attracted much attention due to their magnetic and electric conducting properties.[13−16] For ex-

* To whom correspondence should be addressed. E-mail: mpsuh@snu.ac.kr.

(1) Malinsky, M. D.; Kelly, K. L.; Schatz, G. C.; Duyne, R. P. V. *J. Am. Chem. Soc.* **2001**, *123*, 1471.
(2) Ziegler, K. J.; Doty, R. C.; Johnston, K. P.; Korgel, B. A. *J. Am. Chem. Soc.* **2001**, *123*, 7797.
(3) Ryoo, R.; Park, I. S.; Jun, S.; Lee, C. W.; Kruk, M.; Jaroniec, M. *J. Am. Chem. Soc.* **2001**, *123*, 1650.
(4) Choy, J. H.; Kwon, S. J.; Park, G. S. *Science* **1998**, *280*, 1589.
(5) Cho, B. K.; Lee, M. S. *J. Am. Chem. Soc.* **2001**, *123*, 9677.
(6) Jung, J. H.; Ono, Y.; Sakurai, K.; Sano, M.; Shinkai, S. *J. Am. Chem. Soc.* **2000**, *122*, 8646.
(7) Elliott, J. M.; Chipperfield, J. R.; Clark, S.; Teat, S. J.; Sinn, E. *Inorg. Chem.* **2002**, *41*, 293.
(8) Arulsamy, N.; Bohle, D. S.; Goodson, P. A.; Jaeger, D. A.; Reddy, V. B. *Inorg. Chem.* **2001**, *40*, 836.
(9) Manabe, K.; Mori, Y.; Wakabayashi, T.; Nagayama, S.; Kobayashi, S. *J. Am. Chem. Soc.* **2000**, *122*, 7202.
(10) Kimura, E.; Hashimoto, H.; Koike, T. *J. Am. Chem. Soc.* **1996**, *118*, 10963.
(11) Hay, R. W.; Danby, A.; Lightfoot, P.; Lampeka, Y. D. *Polyhedron* **1997**, *16*, 2777.
(12) Fallis, I. A.; Griffiths, P. C.; Griffiths, P. M.; Hibbs, D. E.; Hursthouse, M. B.; Winnington, A. L. *Chem. Commun.* **1998**, 665.
(13) Broderick, W. E.; Hoffman, B. M. *J. Am. Chem. Soc.* **1991**, *113*, 6334.
(14) Broderick, W. E.; Thompson, J. A.; Day, E. P.; Hoffman, B. M. *Science* **1990**, *249*, 401.
(15) Bryce, M. R.; Murphy, L. C. *Nature* **1984**, *309*, 119.

10.1021/ic025971p CCC: $25.00
Published on Web 01/23/2003

ample, $[Cr(C_5(CH_3)_5)_2][TCNQ]$ and $[Mn(C_5(CH_3)_5)_2][TCNQ]$ complexes form donor−acceptor (D^+A^-) charge-transfer complexes, which behave as bulk ferromagnets.[13,14] The charge-transfer complexes of TTF−TCNQ (TTF = tetrathiafulvalene) show electric conductivity of metallic character.[15,16]

Here, we report nickel(II) macrocyclic complexes containing the 1-hexadecyl alkyl chain, $[Ni(C_{25}H_{55}N_5)](ClO_4)_2 \cdot H_2O$ (**1**) and $[Ni(C_{25}H_{55}N_5)(TCNQ)_2](TCNQ) \cdot (CH_3COCH_3)$ (**2**). Compound **1** shows a hydrophobic effect for the long alkyl chains in the solid state. The insoluble solid **1** exhibits ion exchange ability with various anions in aqueous solutions. In **2**, the TCNQ anions coordinating the nickel(II) macrocycle at the axial sites involve $\pi-\pi$ stacking interactions with those of the adjacent complexes, which gives rise to a 1-D chain. The neutral TCNQ molecules are included between the coordinated TCNQ anions to give rise to a π-stacked group of six TCNQ species as being blocked by the long alkyl chains of the macrocycles. Compound **2** behaves as an electric insulator at room temperature. It exhibits simple paramagnetic behavior at low temperatures (<100 K) arising from the isolated $S = 1$ spins of nickel(II) ion, but the $\chi_M T$ value increases at the higher temperatures because of the contribution of a thermally accessible triplet state for the antiferromagnetically coupled $[TCNQ]_2^{2-}$. To the best of our knowledge, **1** is the first example of a simple transition metal complex that exhibits an anion exchange property in the solid state, even though many layered compounds and metal-organic open frameworks showed ion exchange ability.[17−19] In addition, compound **2** is the first example among metal−TCNQ systems in which the pendant alkyl group of the ligand controls the extent of TCNQ stacking.

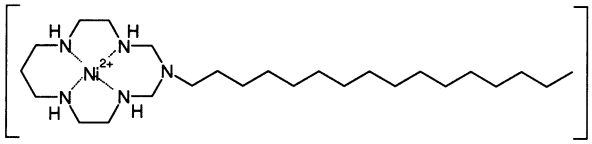

$[Ni(C_{25}H_{55}N_5)]^{2+}$

Experimental Section

Reagents. All chemicals and solvents used in the syntheses were of reagent grade and were used without further purification. For the spectroscopic measurements, water was distilled, and organic solvents were dried over molecular sieves prior to use. $Et_3NH(TCNQ)_2$ was prepared according to the procedure reported previously.[20]

Measurements. Infrared spectra were recorded with a Perkin-Elmer 2000 FT-IR spectrophotometer. Elemental analyses were performed by the analytical laboratory of Seoul National University. UV−vis spectra were recorded on a Cary 300 Bio UV−vis spectrophotometer. X-ray powder diffraction (XRPD) data were obtained by a Mac Science M18XHF-22 diffractometer at 50 kV and 100 mA for Cu Kα (λ = 1.54050 Å) with a scan speed of 5°/min and a step size of 0.02° in 2θ. Magnetic susceptibility was measured by a Quantum Design MPMS superconducting quantum interference device (SQUID). EPR spectra were recorded on a Bruker EPR EMX spectrometer.

Synthesis. $[Ni(C_{25}H_{55}N_5)Cl_2]$. To a stirred MeOH solution (30 mL) of $NiCl_2 \cdot 6H_2O$ (1.4 g, 5.9 mmol) were added *N*,*N*′-bis(2-aminoethyl)-1,3-propanediamine (0.97 g, 6.0 mmol), a methanol solution (20 mL) of 1-hexadecylamine (1.3 g, 5.4 mmol), and 37% aqueous formaldehyde (1.3 g, 16 mmol). The mixture was heated at reflux for 72 h. The solution was filtered while hot, and the filtrate was allowed to stand at room temperature until a pink precipitate formed, which was filtered off, washed with diethyl ether to remove unreacted 1-hexadecylamine, and dried in air. Yield: 38%. The compound is soluble in CH_2Cl_2 and $CHCl_3$ to give pink solutions. It is also soluble in hot alcohols to provide yellow solutions. It is slightly soluble in DMF and insoluble in water. Anal. Calcd for $NiC_{25}H_{55}N_5Cl_2$: C, 54.07; H, 9.98; N, 12.11. Found: C, 53.65; H, 9.84; N, 12.59. FT-IR (Nujol mull, cm^{-1}): ν(NH), 3277, 3262, 3205; ν(C−C), 1466, 1377.

$[Ni(C_{25}H_{55}N_5)](ClO_4)_2 \cdot H_2O$ (1). $[Ni(C_{25}H_{55}N_5)Cl_2]$ (0.65 g, 1.2 mmol) was dissolved in a warm EtOH/H_2O solution (1:1 v/v, 30 mL), and the solution was hot-filtered to remove insoluble solid. An excess amount of $LiClO_4$ (0.84 g, 7.9 mmol) was added to the solution, which immediately produced a yellow microcrystalline solid. The crystals were filtered off, washed with a mixture of EtOH/H_2O (1:1, v/v), and dried in air. Yield: 90%. The compound is soluble in MeCN, alcohols, acetone, DMF, and DMSO but insoluble in water and diethyl ether. To obtain single crystals of **1** for X-ray diffraction study, solid **1** was dissolved in hot EtOH (60 °C), and a few drops of water were added to the solution. The solution was cooled very slowly to room temperature, from which yellow crystals formed in several days. Anal. Calcd for $NiC_{25}H_{55}N_5Cl_2O_8$: C, 43.94; H, 8.11; N, 10.25. Found: C, 44.13; H, 7.88; N, 10.39. FT-IR (Nujol mull, cm^{-1}): ν(NH), 3213; ν(C−C), 1469, 1419, 1375; ν(Cl−O), 1091, 1019, 624. UV−vis in DMF, λ_{max} (ϵ, M^{-1} cm^{-1}): 455 nm (24.6). UV−vis (diffuse reflectance spectrum), λ_{max}: 461 nm.

$[Ni(C_{25}H_{55}N_5)(TCNQ)_2](TCNQ) \cdot (CH_3COCH_3)$ (2). To a hot (60−80 °C) ethanol solution (5.0 mL) of $[Ni(C_{25}H_{55}N_5)Cl_2]$ (42 mg, 0.076 mmol) was slowly added a DMF/acetone (3:5, v/v, 8 mL) solution of $Et_3NH(TCNQ)_2$ (82 mg, 0.16 mmol). The solution was filtered while hot, and the filtrate was allowed to stand at room temperature for 1 day until dark purple crystals formed. The crystals were filtered off, which were immersed in water for a day to remove a small amount of Et_3NHCl salts contaminating the product. The crystals were filtered, washed with EtOH, and dried in air. Yield: 53%. The compound is soluble in DMF, MeCN, and acetone but insoluble in water and alcohols. A single crystal used for the X-ray crystallography was selected from the product. Anal. Calcd for $NiC_{64}H_{73}N_{17}O$: C, 66.55; H, 6.37; N, 20.62. Found: C, 65.83; H, 6.42; N, 20.29. FT-IR (Nujol mull, cm^{-1}): ν(NH), 3261, 3240; ν(CN), 2219, 2190, 2157; ν(C═C), 1582, 1540, 1505; ν(C−C), 1465, 1374; ν(C−H), 840, 826. UV−vis in MeCN, λ_{max} (ϵ, M^{-1} cm^{-1}): 393 nm (111 000), 744 nm (52 600), 843 nm (100 000).

$[Ni(C_{25}H_{55}N_5)(NCS)_2]$ (3). To an MeCN solution (25 mL) of **1** (0.186 g, 0.265 mmol) was added an MeCN solution (5.0 mL) of an excess amount of NaNCS (0.204 g, 2.52 mmol). The solution turned purple, which was concentrated until it became ca. $^1/_3$ of the initial volume. The solution was allowed to stand at room temperature until purple microcrystals formed, which were filtered off, washed with diethyl ether, and dried in air. Yield: 90%. Anal. Calcd for $NiC_{27}H_{55}N_7S_2$: C, 54.00; H, 9.23; N, 16.33; S, 10.66. Found: C, 53.74; H, 8.96; N, 16.11; S, 10.41. FT-IR (Nujol mull,

(16) Jerome, D.; Schulz, H. J. *Adv. Phys.* **2002**, *51*, 293.
(17) Tran, D. T.; Zavalij, P. Y.; Oliver, S. R. *J. Am. Chem. Soc.* **2002**, *124*, 3966.
(18) Yaghi, O. M.; Li, H. *J. Am. Chem. Soc.* **1996**, *118*, 295.
(19) Min, K. S.; Suh, M. P. *J. Am. Chem. Soc.* **2000**, *122*, 6834.
(20) Melby, L. R.; Harder, R. J.; Hertler, W. R.; Mahler, W.; Benson, R. E.; Mochel, W. E. *J. Am. Chem. Soc.* **1962**, *84*, 3374−3387.

cm^{-1}): ν(NH), 3289, 3236; ν(NCS^-), 2057; ν(C−C), 1470, 1420, 1377. UV−vis in DMF, λ_{max} (ϵ, M^{-1} cm^{-1}): 501 nm (10.4). UV−vis (diffuse reflectance spectrum), λ_{max}: 497 and 685 nm.

[Ni($C_{25}H_{55}N_5$)](PF_6)$_2$ (4). To an MeCN solution (15 mL) of **1** (0.179 g, 0.255 mmol) was added an MeCN solution (5.0 mL) of an excess amount of NH_4PF_6 (0.411 g, 2.52 mmol). The solution turned to yellow-green, and white precipitate NH_4ClO_4 formed, which was filtered off. The solution was concentrated until pale green microcrystals formed, which were filtered, washed with a mixture of EtOH/H_2O (1:5, v/v) and then diethyl ether, and dried in air to obtain yellow crystals. Yield: 94%. Anal. Calcd for $NiC_{25}H_{55}N_5P_2F_{12}$: C, 38.77; H, 7.16; N, 9.00. Found: C, 38.23; H, 7.09; N, 8.98. FT-IR (Nujol mull, cm^{-1}): ν(NH), 3242; ν(C−C), 1459, 1419, 1376; ν(P−F), 833. UV−vis in MeCN, λ_{max} (ϵ, M^{-1} cm^{-1}): 465 nm (13.3). Although the single crystal of **4** diffracted the X-ray beam, the X-ray data quality was not good enough to determine the structure. Cell parameters: a = 8.866(5) Å, b = 8.869 (5) Å, c = 28.164 (5) Å, α = 96.051 (5)°, β = 93.940 °, γ = 116.896 (5)°, Z = 2, V = 1946.92 (29) Å^3.

Ion Exchange of 1 in the Solid State. To examine if **1** shows anion exchange ability, freshly prepared yellow microcrystals of **1** (0.25 g) were immersed in the aqueous solution (1.0 M, 10 mL) of NaNCS for 3 h. Solid **1** was also immersed in the aqueous solution of NH_4PF_6 (1.0 M, 10 mL) for 1 day as well as in the aqueous solutions of $LiCF_3SO_3$ (0.92 M, 10 mL), $NaNO_3$ (1.2 M, 10 mL), and $Na_2C_2O_4$ (0.19 M, 50 mL), respectively, for 2 days. Because the solid repels water and floats on the aqueous solution because of hydrophobicity of the long alkyl chain, the solution was sonicated for several minutes and then allowed to stand at room temperature for the rest of the time. When **1** was immersed in the aqueous solution (1.0 M, 10 mL) of NaNCS, the solution was sonicated over 1 h. The resulting anion-exchanged solid was filtered off, washed with the mixture of water and EtOH (1:1, v/v) and then with diethyl ether, and dried in air. The products were characterized by elemental analyses (EA), FT-IR, and XRPD patterns. The EA data for the anion exchanged solids follow. Anal. Calcd for [Ni($C_{25}H_{55}N_5$)($NCS)_2$] ($NiC_{27}H_{55}N_7S_2$): C, 54.00; H, 9.23; N, 16.33; S, 10.66. Found: C, 53.42; H, 6.78; N, 15.70; S, 8.60. ν(NCS^-): 2057 cm^{-1}. UV−vis (diffuse reflectance spectrum), λ_{max}: 489 and 685 nm. Anal. Calcd for [Ni($C_{25}H_{55}N_5$)](PF_6)$_2$(H_2O)$_{1.5}$ ($NiC_{25}H_{58}N_5O_{1.5}P_2F_{12}$): C, 37.46; H, 6.917; N, 8.739. Found: C, 37.23; H, 5.07; N, 8.759. ν(OH): 3564 cm^{-1}. ν(PF_6^-): 833 cm^{-1}. Anal. Calcd for [Ni($C_{25}H_{55}N_5$)](CF_3SO_3)$_{0.3}$(ClO_4)$_{1.7}$ ($NiC_{25.3}H_{55}N_5O_{7.7}F_{0.9}S_{0.3}Cl_{1.7}$): C, 43.52; H, 7.94; N, 10.03; S, 1.37. Found: C, 43.38; H, 6.94; N, 10.00; S, 0.488. ν(SO_3^-): 1282 cm^{-1}. Anal. Calcd for [Ni($C_{25}H_{55}N_5$)](NO_3)$_{0.3}$(ClO_4)$_{1.7}$ ($NiC_{25}H_{55}N_{5.3}O_{7.7}Cl_{1.7}$): C, 44.67; H, 8.25; N, 11.05. Found: C, 44.54; H, 7.01; N, 11.02. ν(NO_3^-): 1304 cm^{-1}. Anal. Calcd for [Ni($C_{25}H_{55}N_5$)(SO_4)$_{0.2}$](ClO_4)$_{1.6}$(H_2O) ($NiC_{25}H_{57}N_5O_{8.2}S_{0.2}Cl_{1.6}$): C, 44.11; H, 8.44; N, 10.29; S, 0.94. Found: C, 44.07; H, 6.03; N, 10.35; S, 0.985. ν(OH): 3600 cm^{-1}, ν(SO_4^-): 1097, 1023 cm^{-1}. Anal. Calcd for [Ni($C_{25}H_{55}N_5$)(C_2O_4)$_{0.5}$](ClO_4)(H_2O)$_{1.5}$ ($NiC_{26}H_{58}N_5O_{7.5}Cl$): C, 47.68; H, 8.93; N, 10.69. Found: C, 47.98; H, 7.41; N, 10.76. ν(OH): 3400 cm^{-1}, ν(COO): 1643, 1573, 1316 cm^{-1}. To check the reversibility of **1** for the anion exchange, freshly prepared solids of [Ni($C_{25}H_{55}N_5$)($NCS)_2$] (**3**) (0.102 g) and [Ni($C_{25}H_{55}N_5$)](PF_6)$_2$ (**4**) (0.125 g), respectively, were immersed in the aqueous solutions (3.0 M, 10 mL) of $LiClO_4$ for 4 days. Because the solid floats on the solution, the mixture was sonicated for several minutes and then allowed to stand at room temperature for the rest of time. The resulting anion-exchanged solid was filtered off, washed with the mixture of water and EtOH (1:1, v/v), and dried in air. The products were characterized by EA and FT-IR, which indicated partial ion exchange. The XRPD patterns of the resulting products were compared with that of **1**. Anal. Calcd for [Ni($C_{25}H_{55}N_5$)($NCS)_{1.8}$](ClO_4)$_{0.2}$ ($NiC_{26.8}H_{55}N_{6.8}O_{0.8}S_{1.8}Cl_{0.2}$): C, 52.87; H, 9.11; N, 15.65; S, 9.46. Found: C, 53.49; H, 9.33; N, 16.03; S, 9.08. ν(ClO_4): 1095 cm^{-1}. Anal. Calcd for [Ni($C_{25}H_{55}N_5$)](PF_6)$_{0.6}$(ClO_4)$_{1.4}$ ($NiC_{25}H_{55}N_5O_{5.6}P_{0.6}F_{3.6}Cl_{1.4}$): C, 42.25; H, 7.80; N, 9.85. Found: C, 42.36; H, 7.94; N, 9.86. ν(ClO_4): 1097 cm^{-1}.

Table 1. Crystallographic Data for [Ni($C_{25}H_{55}N_5$)](ClO_4)$_2$·(H_2O) (**1**) and [Ni($C_{25}H_{55}N_5$)($TCNQ)_2$]($TCNQ$)·(CH_3COCH_3) (**2**)

	1	**2**
empirical formula	$NiC_{25}H_{57}N_5Cl_2O_9$	$NiC_{64}H_{73}N_{17}O$
fw	701.37	1155.10
space group	$P\bar{1}$, triclinic	$P\bar{1}$, triclinic
a, Å	8.333(4)	8.459(0)
b, Å	8.356(3)	13.945(1)
c, Å	28.374(9)	26.833(2)
α, deg	81.865(19)	88.744(2)
β, deg	86.242(18)	84.536(2)
γ, deg	63.871(17)	80.089(4)
V, Å^3	1755.9(12)	3103.8(3)
Z	2	2
ρ_{calcd}, g cm^{-3}	1.327	1.236
T, K	293(2)	293(2)
λ, Å	0.710 73	0.710 73
μ, mm^{-1}	0.756	0.368
GOF	0.983	0.935
F(000)	752	1224
no. data collected	3230	15818
no. unique data	2829	10410
no. variables	380	746
R^a (4σ data)	0.0851	0.0757
$R_w(F^2)$ (4σ data)	0.2144[b]	0.1770[c]
largest peak and hole (e/Å^3)	0.478, −0.317	0.541, −0.816

[a] $R = \sum||F_o| - |F_c||/\sum|F_o|$. [b] R_w (F^2) = $[\sum w(F_o^2 - F_c^2)^2/\sum w(F_o^2)^2]^{1/2}$ where $w = 1/[\sigma^2(F_o^2) + (0.1447P)^2 + 0.0000P]$, $P = (F_o^2 + 2F_c^2)/3$ for **1**. [c] R_w (F^2) = $[\sum w(F_o^2 - F_c^2)^2/\sum w(F_o^2)^2]^{1/2}$ where $w = 1/[\sigma^2(F_o^2) + (0.1123P)^2 + 0.0000P]$, $P = (F_o^2 + 2F_c^2)/3$ for **2**.

X-ray Crystallography. Diffraction data for **1** and **2** were collected with an Enraf Nonius Kappa CCD diffractometer (Mo Kα, λ = 0.71073 Å, graphite monochromator). Preliminary orientation matrices and unit cell parameters were obtained from the peaks of the first 10 frames and then refined using the whole data set. Frames were integrated and corrected for Lorentz and polarization effects using DENZO.[21] The scaling and the global refinement of crystal parameters were performed by SCALEPACK.[21] No absorption correction was made. The crystal structures were solved by the direct methods[22] and refined by full-matrix least-squares refinement using the SHELXL-97 computer program.[23] The positions of all non-hydrogen atoms were refined with anisotropic displacement factors. The hydrogen atoms were positioned geometrically and refined using a riding model. The crystallographic data of **1** and **2** are summarized in Table 1.

Results and Discussion

Synthesis and X-ray Structure of 1. The nickel(II) macrocyclic complex containing the 1-hexadecyl pendant group, [Ni($C_{25}H_{55}N_5$)](ClO_4)$_2$·H_2O (**1**), was synthesized by the one-pot template condensation reaction of *N*,*N*′-bis(2-

(21) Otwinowsky, Z.; Minor, W. *Processing of X-ray Diffraction Data Collected in Oscillation Mode, Methods in Enzymology*; Carter, C. W., Sweet, R. M., Eds.; Academic Press: New York, 1996; Vol. 276, pp 307−326.
(22) Sheldrick, G. M. *Acta Crystallogr*. **1990**, *A46*, 467.
(23) Sheldrick, G. M. *SHELXL97, Program for the Crystal Structure Refinement*; University of Göttingen: Göttingen, Germany, 1997.

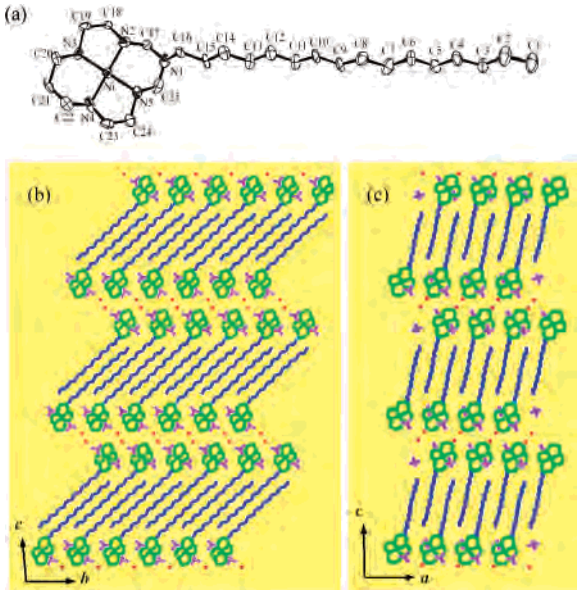

Figure 1. (a) ORTEP drawing of the asymmetric unit of **1** with atomic numbering scheme. Thermal ellipsoids are drawn with 30% probability. Packing structures of **1** showing hydrophobic layers: (b) a view on the *bc* plane and (c) a view on the *ac* plane. Green, macrocycle; blue, alkyl pendant chain; purple, perchlorate anion; red, water molecule.

aminoethyl)-1,3-propanediamine, formaldehyde, and 1-hexadecylamine in the presence of nickel(II) ion. The metal-template condensation reaction of amines and formaldehyde has been well established in our laboratory.[24−26] Compound **1** is soluble in DMF, Me_2SO, MeCN, and $MeNO_2$, and in hot alcohols, but it is completely insoluble in water as evidenced by the NMR spectrum measured in D_2O. Compound **1** floats on the surface of water although its density is greater than 1.0, because of the hydrophobicity of the compound.

An ORTEP drawing for the cation and a packing structure of **1** are shown in Figure 1. Table 2 shows selected bond distances and angles. Compound **1** consists of two parts, the metal headgroup with macrocycle and the hydrophobic alkyl pendant chain. The estimated size of the headgroup is ca. 9.4×8.8 Å^2, and that of the tail is ca. 21 Å. The nickel(II) ion displays a square-planar coordination geometry by binding four secondary nitrogen donors of the macrocycle with an average Ni−N bond distance of 1.946(4) Å. The ClO_4^- anions are not coordinated to the nickel(II) ion. The Ni···O(perchlorate) distances are 2.768(13) and 2.986(12) Å, which are too long to be considered as bonds as compared with the reported Ni−O bond distances (2.089−2.301 Å) for the six-coordinate nickel(II) complexes of tetraaza ligands.[27] In the crystal structure, the complexes are packed, facing the headgroups to the opposite side of one another and gathering the tail groups together, which constructs a thick hydrophobic layer (Figure 1b). Because the hydrophobic effect of the long aliphatic chains leads to close packing

Table 2. Selected Bond Distances (Å) and Angles (deg) of **1**[a]

Ni1−N3	1.936(8)	C6−C7	1.55(2)	N3−Ni1−N5	177.5(4)
Ni1−N4	1.953(10)	C7−C8	1.533(15)	N4−Ni1−N5	86.6(4)
Ni1−N5	1.956(8)	C8−C9	1.524(19)	N3−Ni1−N2	85.6(4)
Ni1−N2	1.957(11)	C9−C10	1.517(16)	N4−Ni1−N2	179.1(4)
Ni1−O3	2.768(13)	C10−C11	1.490(17)	N5−Ni1−N2	92.5(4)
Ni1−O5′	2.986(12)	C11−C12	1.518(15)	N2−Ni1−O3	96.2(4)
N1−C25	1.393(16)	C12−C13	1.603(18)	N3−Ni1−O3	97.5(4)
N1−C17	1.416(14)	C13−C14	1.552(15)	N3−Ni1−N4	95.3(4)
N1−C16	1.425(15)	C14−C15	1.487(17)	N4−Ni1−O3	83.5(4)
N2−C18	1.464(13)	C15−C16	1.541(15)	N5−Ni1−O3	84.2(4)
N2−C17	1.504(15)	C18−C19	1.494(17)	N2−Ni1−O5′	84.2(4)
N3−C19	1.489(13)	C20−C21	1.490(17)	N3−Ni1−O5′	85.0(4)
N3−C20	1.507(16)	C21−C22	1.486(18)	N4−Ni1−O5′	95.9(4)
N4−C22	1.482(16)	C23−C24	1.426(19)	N5−Ni1−O5′	93.2(4)
N4−C23	1.493(15)	Cl1−O1	1.350(11)		
N5−C25	1.522(18)	Cl1−O4	1.380(10)		
N5−C24	1.530(16)	Cl1−O3	1.463(12)		
C1−C2	1.477(18)	Cl1−O2	1.503(13)		
C2−C3	1.603(19)	Cl2−O6	1.339(11)		
C3−C4	1.522(15)	Cl2−O5	1.374(10)		
C4−C5	1.517(17)	Cl2−O8	1.389(14)		
C5−C6	1.464(14)	Cl2−O7	1.441(12)		

[a] Symmetry transformations used to generate equivalent atoms: prime, $x, y + 1, z$.

of the pendant hexadecyl groups,[28] the distance between two adjacent chains is 4.2 Å (from C9 of a chain to the nearest carbon atom of the adjacent chain). The interactions between the pendant chains extend along both *a* and *b* axes. The ClO_4^- anions and lattice water molecules are positioned between the metal headgroups.

Anion Exchange Property of 1. When insoluble solid **1** was immersed in the aqueous solution of 1.0 M NaNCS for 3 h with 1 h of sonication, the yellow color of the solid turned to pale pink, indicating that nickel(II) ion in **1** was coordinated with NCS^- anions. The anion exchange of ClO_4^- in **1** with NCS^- was verified by elemental analysis and FT-IR, which indicated more than 95% exchange, as well as by UV−vis diffuse reflectance spectra. The FT-IR spectrum shows a new peak at 2057 cm^{-1}, which corresponds to the coordinated NCS^- anions.[29] The UV−vis reflectance spectrum showed maximum absorption at 489 and 685 nm, indicative of five- or six-coordinated nickel(II) ion.[30] In addition, the XRPD patterns for the ion-exchanged product showed those of $[Ni(C_{25}H_{55}N_5)(NCS)_2]$ (**3**), which was prepared independently from the MeCN solutions of **1** and NaNCS, although they still contained patterns of **1** (Figure 2). The XRPD of the ion-exchanged solid also implied that the structure of **1** was transformed to that of **3** by anion exchange in the solid state.[19] However, when the solution was sonicated for a shorter period of time, only a small percentage of the ClO_4^- anions in **1** was exchanged with NCS^- even after 24 h, as evidenced by XRPD patterns as well as elemental analysis data (see Supporting Information).

Similarly, the ClO_4^- anion of **1** was also exchanged with PF_6^- in the crystalline state, as verified by the elemental

(24) Suh, M. P.; Kang, S. K. *Inorg. Chem.* **1988**, *27*, 2544.
(25) Suh, M. P. *Adv. Inorg. Chem.* **1996**, *44*, 93−146.
(26) Suh, M. P.; Shim, B. Y.; Yoon, T. S. *Inorg. Chem.* **1994**, *33*, 5509.
(27) CSD database released on April, 2002. Allen, F. H.; Kennard, O. *Chemical Design Automation News* **1993**, *8* (1), 1 and 31−37.
(28) Desiraju, G. *Crystal Engineering: The Design of Organic Solids*; Elsevier: New York, 1989; pp 89−92.
(29) Nakamoto, K. *Infrared and Raman Spectra of Inorganic and Coordination Compounds*, 4th ed.; Wiley & Sons: New York, 1986; pp 283−287.
(30) Melson, G. A. *Coordination Chemistry of Macrocyclic Compounds*; Plenum Press: New York, 1979; pp 349−350.

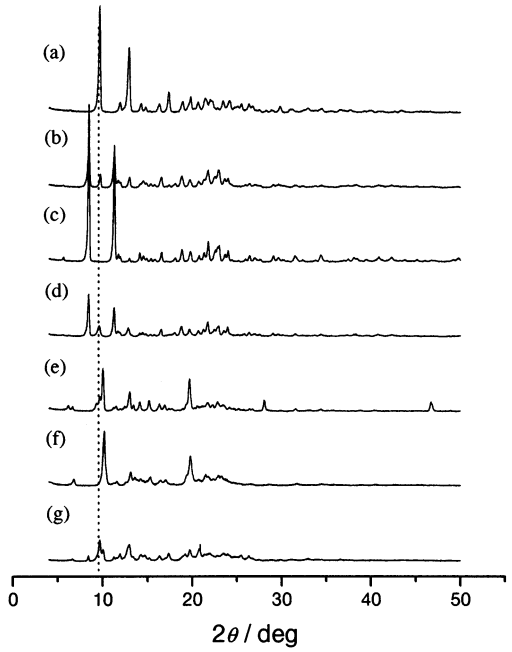

Figure 2. XRPD patterns for anion-exchanged solids: (a) the original host solids **1**, (b) **1** immersed in aq NaNCS (1.0 M) solution for 3 h with 1 h of sonication, (c) $[Ni(C_{25}H_{55}N_5)(NCS)_2]$ as synthesized, (d) sample in part c immersed in aq $LiClO_4$ (3.0 M) solution for 4 days, (e) **1** immersed in aq NH_4PF_6 (0.9 M) solution for 1 day, (f) $[Ni(C_{25}H_{55}N_5)](PF_6)_2$ as synthesized, (g) sample in part f immersed in aq $LiClO_4$ (3.0 M) solution for 4 days.

analysis and FT-IR spectrum. The XRPD pattern of the ion-exchanged product was coincident with that of $[Ni(C_{25}H_{55}N_5)](PF_6)_2$ (**4**), which was prepared independently from the MeCN solutions of **1** and NH_4PF_6 (see Experimental Section). However, when solid **1** was immersed in the aqueous solutions of 0.92 M $LiCF_3SO_3$, 1.2 M $NaNO_3$, 1.0 M $NiSO_4 \cdot 6H_2O$, and 0.2 M $Na_2C_2O_4$, respectively, for 2 days, the ClO_4^- anions in **1** were only partially (15−20%) exchanged with the corresponding anions. The anion exchange was reversible. When the solids $[Ni(C_{25}H_{55}N_5)(NCS)_2]$ (**3**) and $[Ni(C_{25}H_{55}N_5)](PF_6)_2$ (**4**), respectively, were immersed in the aqueous solutions of $LiClO_4$ (3.0 M) for 4 days, 1% of **3** and 70% of **4** were ion-exchanged with ClO_4^-, as identified by EA and FT-IR spectra. Because PF_6^- and ClO_4^- anions have similar size and shape, they probably exchange each other easily. However, in the case of **3**, exchange of NCS^- with ClO_4^- should involve dissociation of the nickel(II)−NCS bonds, and it cannot be so easy. The anion exchange results in the aqueous media where solid **1** is insoluble indicate that the anion affinity of host **1** is related to the coordination ability of the anion. For example, $C_2O_4^{2-}$ anion is able to coordinate nickel(II) ion, and it replaces 50% of ClO_4^- of **1** even in the more dilute solution (0.2 M) in 2 days.

Synthesis and X-ray Structure of 2. The TCNQ derivative of the macrocyclic complex with a long alkyl chain, $[Ni(C_{25}H_{55}N_5)(TCNQ)_2](TCNQ)\cdot(CH_3COCH_3)$ (**2**), was obtained from the reaction of an EtOH solution of $[Ni(C_{25}H_{55}N_5)Cl_2]$ with an EtOH/DMF/acetone solution of $Et_3NH(TCNQ)_2$. An ORTEP drawing of the cation and a packing structure for **2** are presented in Figure 3. Table 3 shows selected bond distances and angles. In **2**, the nickel(II) ion of the macrocyclic complex is coordinated with two

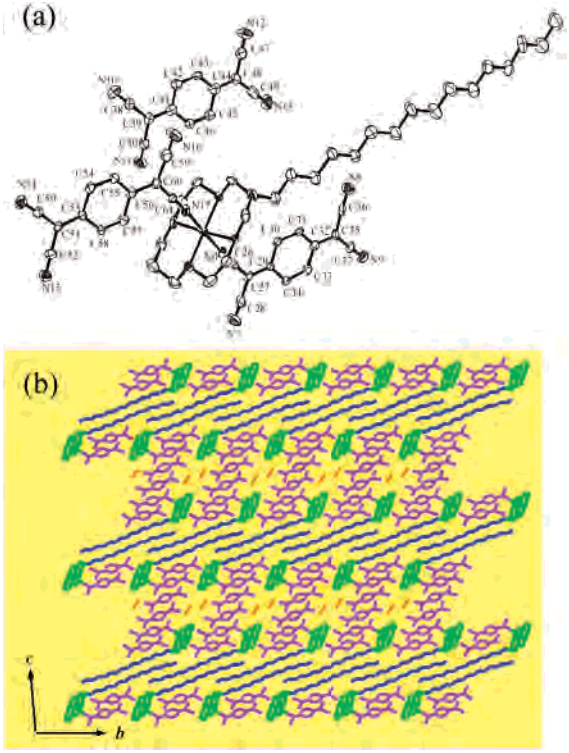

Figure 3. (a) ORTEP drawing of the asymmetric unit of **2** with atomic numbering scheme. Thermal ellipsoids are drawn with 30% probability. (b) Packing diagram of **2** showing stacked TCNQ molecules grouped by six units. Purple, TCNQ; orange, acetone; other colors are the same as in Figure 1.

Table 3. Selected Bond Distances (Å) and Angles (deg) of **2**

Ni1−N2	2.065(7)	N11−C40	1.140(10)	N2−Ni1−N3	85.6(3)
Ni1−N3	2.080(6)	N12−C47	1.081(10)	N2−Ni1−N5	93.3(3)
Ni1−N5	2.081(6)	N13−C49	1.123(13)	N3−Ni1−N5	178.6(3)
Ni1−N4	2.085(6)	C38−C39	1.477(13)	N2−Ni1−N4	177.7(3)
Ni1−N6	2.177(8)	C39−C41	1.355(11)	N3−Ni1−N4	95.2(3)
Ni1−N17	2.214(8)	C39−C40	1.442(12)	N5−Ni1−N4	85.9(3)
N1−C16	1.453(11)	C41−C46	1.461(12)	N2−Ni1−N6	90.7(3)
N1−C25	1.454(10)	C41−C42	1.474(11)	N3−Ni1−N6	91.2(3)
N1−C17	1.467(11)	C42−C43	1.335(11)	N5−Ni1−N6	89.7(3)
N2−C17	1.473(10)	C43−C44	1.457(12)	N4−Ni1−N6	91.4(3)
N2−C18	1.499(10)	C44−C48	1.386(12)	N2−Ni1−N17	89.5(3)
N3−C19	1.490(10)	C44−C45	1.495(11)	N3−Ni1−N17	88.2(3)
N3−C20	1.535(10)	C45−C46	1.293(11)	N5−Ni1−N17	90.9(3)
N4−C23	1.498(10)	C47−C48	1.517(13)	N4−Ni1−N17	88.4(3)
N4−C22	1.519(9)	C48−C49	1.459(15)	N6−Ni1−N17	179.3(3)
N5−C25	1.486(9)	N14−C50	1.151(11)		
N5−C24	1.508(9)	N15−C52	1.109(9)		
C2−C3	1.495(15)	N16−C59	1.103(10)		
N6−C26	1.172(11)	N17−C61	1.166(10)		
N7−C28	1.134(9)	C50−C51	1.429(13)		
N8−C36	1.152(9)	C51−C53	1.377(11)		
N9−C37	1.131(10)	C51−C52	1.446(11)		
C26−C27	1.422(13)	C53−C58	1.399(10)		
C27−C29	1.410(11)	C53−C54	1.433(10)		
C27−C28	1.472(12)	C54−C55	1.342(10)		
C29−C30	1.403(9)	C55−C56	1.402(11)		
C29−C34	1.431(11)	C56−C60	1.423(11)		
C30−C31	1.338(10)	C56−C57	1.463(10)		
C31−C32	1.417(11)	C57−C58	1.325(10)		
C32−C35	1.396(11)	C59−C60	1.472(12)		
C32−C33	1.411(10)	C60−C61	1.382(12)		
C33−C34	1.367(10)	O1−C62	1.166(10)		
C35−C37	1.425(12)	C62−C63	1.434(13)		
C35−C36	1.456(12)	C62−C64	1.501(15)		
N10−C38	1.113(11)				

Table 4. Comparison of Bond Distances (Å) of TCNQ in **2** and [Cu(cyclam)(TCNQ)$_2$](TCNQ)

species	*a*	*b*	*c*	*d*	*e*	*b* − *c*	*c* − *d*	*c*/(*b* + *d*)	ref
TCNQ	1.345	1.448	1.374	1.441	1.140	0.074	−0.0067	0.476	31
TCNQ$^-$	1.374	1.423	1.420	1.416	1.153	0.003	0.004	0.500	32
[Cu(cyclam)(TCNQ)$_2$](TCNQ)									
TCNQ$^-$	1.356	1.420	1.400	1.417	1.142	0.020	−0.017	0.494	30
TCNQ	1.324	1.447	1.358	1.438	1.133	0.089	−0.080	0.471	30
2									
TCNQ[a]	1.314	1.472	1.371	1.474	1.114	0.101	−0.103	0.465	*b*
TCNQ^{-a}	1.343	1.420	1.402	1.438	1.140	0.018	−0.036	0.491	*b*

[a] The average value is used. [b] This work.

TCNQ$^-$ anions at the axial sites to display a distorted octahedral coordination geometry. The average Ni−N(axial) bond distance is 2.195(6) Å, which is considerably longer than the Ni−N(macrocycle) bond distances, which average 2.056(4) Å. The dihedral angles between the macrocyclic coordination plane and two TCNQ$^-$ planes are 77.37(19)° and 75.57(18)°, respectively. In **2**, there exist $\pi-\pi$ interactions between the coordinated TCNQ$^-$ ions of the neighboring complexes to form $[TCNQ]_2^{2-}$ dimeric units, which give rise to 1-D chains extending parallel to the *b* axis. The overlapping of the coordinated TCNQ$^-$ ions occurs in the ring over external bond mode.[31] The shortest C···C distance and the dihedral angle between the π-stacked TCNQ$^-$ anions are 3.166(11) Å and 1.87(39)°, respectively. Two neutral TCNQ molecules are inserted between two $[TCNQ]_2^{2-}$ dimeric units with the inversion center between them, and they exhibit $\pi-\pi$ stacking interactions in the ring over external bond mode along the *c* direction, with each other (shortest intermolecular distance, 3.570(17) Å; dihedral angle, 0.00(39)°) as well as with the coordinated TCNQ$^-$ anions (shortest intermolecular distance, 3.315(11) Å; dihedral angle, 7.71(39)°).

The bond distances of TCNQ can be related to the degree of charge held on it.[31,32] The reduced radical anion of TCNQ partially occupies an antibonding orbital, which is reflected in a shortening of *b* and *d* bonds and a lengthening of *c* bonds, which make differences of $b - c$ and $c - d$ be lowered. The degree of charge transfer to the TCNQ can be also related with the $c/(b + d)$ ratio. In Table 4, the distances of TCNQ moieties in **2** are compared with those of [Cu^{II}(cyclam)(TCNQ)$_2$]TCNQ that contains coordinated dimers of $[TCNQ]_2^{2-}$ as well as neutral TCNQ. It clearly shows that the present compound **2** contains coordinated dimers of $[TCNQ]_2^{2-}$ and a neutral TCNQ molecule.

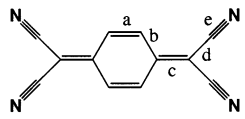

Previously, M(II)(N$_4$)−TCNQ systems (N$_4$ = tetraaza-macrocyclic ligand) have been prepared, and the electronic and magnetic properties were examined.[31,32,35−37] In these systems, 1-D chains of [M(N$_4$)]−(TCNQ)$_2$−[M(N$_4$)]−(TCNQ)$_2$ are formed by the dimerization of coordinated TCNQ$^-$ anions. In particular, the complexes [Cu^{II}(cyclam)-(TCNQ)$_2$](TCNQ),[32] [Fe^{III}(cyclam)(NCS)$_2$](TCNQ)$_2$,[35] [M(dieneN$_4$)](TCNQ)$_3$ (M = Ni(II), Cu(II) and dieneN$_4$ = *cis*- or *trans*-hexamethyltetraazadydlotetradecadiene),[36] and [M(tz)$_2$](TCNQ)$_7$ (M = Ni(II), Cu(II) and tz = 2,7,12,17-tetramethyl-1,6,11,16-tetraazaporphyrinogen)[37] contain neutral TCNQ molecules that are included between the $[TCNQ]_2^{2-}$ dimeric units, which give rise to infinite 1-D π-stacked TCNQ columns. However, in the structure of **2**, TCNQ stacking is limited to a group of six TCNQ units involving four coordinated TCNQ$^-$ anions and two neutral TCNQ molecules, because long alkyl chains of the macrocycles block the infinite π-stacking interactions of the TCNQ species (Figure 3). Compound **2** is the first example, among M(N$_4$)−(TCNQ) systems, in which the extent of TCNQ stacking is controlled by the pendant group of the macrocycle.

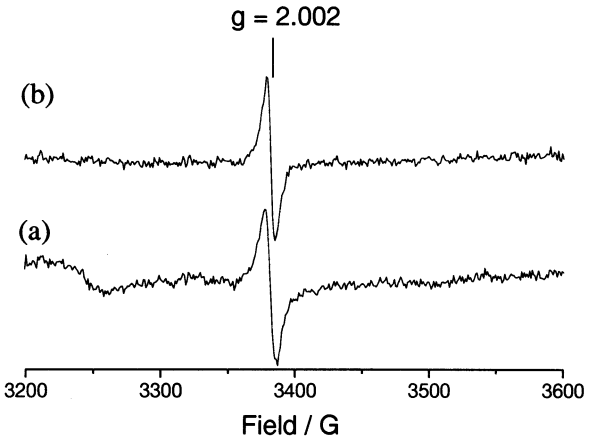

Figure 4. EPR spectra of powder sample of **2** measured (a) at room temperature and (b) at 100 K.

Physical Properties of 2. The infrared spectrum is diagnostic for the formal oxidation state and the coordinative status of the TCNQ molecules.[31] The infrared spectrum of **2** shows that the compound contains coordinated anionic TCNQ$^-$ as well as neutral TCNQ species. The anionic radical TCNQ that is dimerized by the $\pi-\pi$ interaction, $[TCNQ]_2^{2-}$, shows the bands ν(CN) at 2190 and 2157 cm^{-1}, ν(CC) at 1582 and 1505 cm^{-1}, and δ(CH) at 826 cm^{-1}. The neutral TCNQ species shows bands ν(CN) at 2219 cm^{-1}, ν(CC) at 1540 cm^{-1}, and δ(CH) at 840 cm^{-1}.[31]

A powder sample of **2** shows a weak EPR signal at g = 2.002 (Figure 4). The peak intensity does not change significantly even at 100 K. This indicates that the unpaired

(31) Ballester, L.; Gutiérrez, A.; Perpiñán, M. F.; Azcondo, M. T. *Coord. Chem. Rev.* **1999**, *190*−*192*, 447−470.
(32) Ballester, L.; Gil, A. M.; Gutierres, A.; Perpiñán, M. F.; Azcondo, M. T.; Sanchez, A. E.; Amador, U.; Campo, J.; Palacio, F. *Inorg. Chem.* **1997**, *36*, 5291.
(33) Kistenmacher, T. S.; Phillips, J. E.; Cowan, D. O. *Acta Crystallogr., Sect. B* **1974**, *30*, 763.
(34) Hoeskstra, A.; Spoelder, T.; Vos, A. *Acta Crystallogr., Sect. B* **1972**, *28*, 14.
(35) Ballester, L.; Gutiérrez, A.; Perpiñán, M. F.; Rico, S. *Inorg. Chem.* **1999**, *38*, 4430.
(36) Ballester, L.; Gil, A. M.; Gutiérrez, A.; Perpiñán, M. F. *Inorg. Chem.* **2000**, *39*, 2837.
(37) Ballester, L.; Gil, A. M.; Gutiérrez, A.; Perpiñán, M. F.; Azcondo, M. T.; Sanchez, A. E.; Marzin, C.; Tarrago, G.; Bellito, C. *Chem. Eur. J.* **2002**, *8*, 2539.

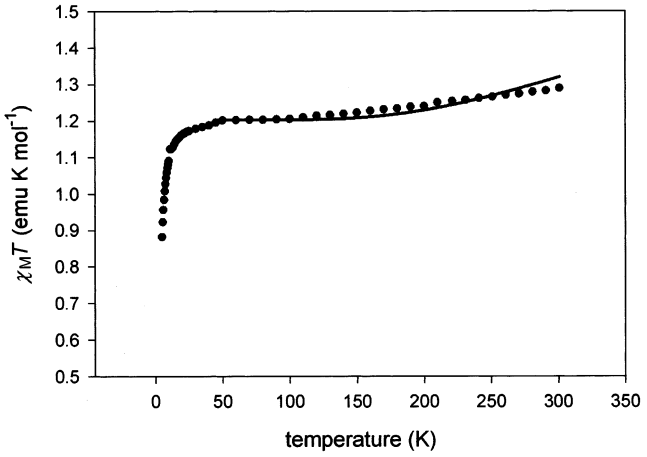

Figure 5. Plot of $\chi_M T$ vs T for **2** under 0.1 T. The solid line represents a curve fit to eq 1 in the temperature range $45 < T < 300$ K.

electron in the $TCNQ^-$ radical anion is paired with that of the adjacent $TCNQ^-$ anion to form dimerized TCNQ units, $[TCNQ]_2^{2-}$. The weak intensity of the EPR spectrum must be attributed to the impurity of nondimerized $TCNQ^-$ radical anions. The similar compound $[Cu^{II}(cyclam)(TCNQ)_2]$-$(TCNQ)$[32] and $[M(tz)_2(MeOH)_2](TCNQ)_2$[37] also exhibited a weak EPR signal arising from the nondimerized $TCNQ^-$ impurities even if $[TCNQ]_2^{2-}$ dimers were formed. However, TCNQ species in the former contributed to the total magnetism while that of the latter was not involved in the magnetic contribution.

The electric resistivity value for the pressed powder sample of **2** is several 10 MΩ at room temperature. This indicates that compound **2** is an electric insulator. It has been reported that two requirements, the formation of infinite TCNQ stacks and the partial reduction of TCNQ molecules to give noninteger oxidation states, should be met to obtain a good low dimensional electrical conductor from TCNQ derivatives.[31] However, in the present complex **2**, negative charge is localized at the TCNQ unit coordinating the metal ion. In addition, only limited numbers of TCNQ species are stacked because of the long alkyl chain of the macrocycle.

The magnetic susceptibility of **2** was measured as a function of temperature at 5−300 K, and the $\chi_M T$ versus T plot is presented in Figure 5. At low temperatures, the $\chi_M T$ versus T values follow the Curie−Weiss law ($\chi = C/[T - \theta]$) with Curie constant $C = 1.223(2)$ emu K mol^{-1} and Weiss temperature $\theta = -1.231(9)$ K, which is attributable to the paramagnetic nickel(II) ions. The effective magnetic moment is 3.10 μ_B at 60 K (3.09 at 45 K to 3.10 at 100 K), which is in the range of commonly observed values for a high spin nickel(II) ion (2.83−3.50 μ_B).[33] However, on raising the temperature, a small increase in the $\chi_M T$ value occurs, from 1.195 emu K mol^{-1} at 45 K to 1.288 emu K mol^{-1} at 300 K, which indicates the existence of a second paramagnetic contribution. This contribution must be due to the presence of a thermally accessible triplet state for the antiferromagnetically coupled $[TCNQ]_2^{2-}$ as a consequence of the weakening in the antiferromagnetic coupling caused by the neutral TCNQ molecules. The molar magnetic susceptibility data in the temperature range 45−300 K were fit to the sum of the Curie and Bleaney−Bowers equation,[32,39] where N, g_{Ni}, g, μ_B, k_B, S, and J represent, respectively, Avogadro's number, g value of nickel(II), g value of TCNQ, Bohr magneton, Boltzmann constant, spin number for high spin nickel(II) ion ($S = 1$), and the coupling constant for interacting TCNQ pairs.

$$\chi_M = \frac{N g_{Ni}^2 \mu_B^2}{3k_B T} S(S+1) + \frac{N g^2 \mu_B^2}{k_B T}\left[\frac{2}{3 + \exp(-2J/k_B T)}\right] \quad (1)$$

The best fit to eq 1 provides $J = -326(7)$ cm^{-1} and $g_{Ni} = 2.193(1)$ when the g value of TCNQ was fixed as 2.002.

Conclusion

The long alkyl chain attached to the nickel(II) macrocyclic complex provides a remarkable effect on the structure and physical and chemical properties of the compound. It provides a water repellant property to the compound. By the formation of hydrophobic layers between the long alkyl chains, the compound is able to show anion exchange ability in the solid state. In the TCNQ derivatives, the long alkyl chain blocks the infinite π-interactions for the TCNQ species, which affects the magnetic and electric-conducting properties. The results imply that we can tune the properties of the complexes by utilizing alkyl chains attached to the ligand. This paper reports compound **1** as the first example of a simple transition metal complex exhibiting an anion exchange property in the solid state and **2** as the first example of the pendant alkyl group of the ligand controlling the extent of TCNQ stacking.

Acknowledgment. This work was supported by the Korea Research Foundation (R01-1999-000-00041-0) and the Center for Molecular Catalysis. Dr. Choi thanks the Ministry of Education, Republic of Korea, for financial support through the Brain Korea 21 program.

Supporting Information Available: NMR spectrum of **1** in D_2O, IR and UV−vis spectra of **2**, the IR spectra, XRPD patterns, and elemental analysis data for the anion-exchanged solids, and the X-ray crystallographic files of **1** and **2** in CIF format. This material is available free of charge via the Internet at http://pubs.acs.org.

IC025971P

(38) Huheey, J. E.; Keiter, E. A.; Keiter, R. L. *Inorganic Chemistry*, 4th ed.; Harper Collins: New York, 1993; p 465.
(39) Kahn, O. *Molecular Magnetism*; VCH: New York, 1993; pp 9−10 and 103−105.